Journal of Coordination Chemistry
Publication details, including instructions for authors and subscription information:
http://www.tandfonline.com/loi/gcoo20

Syntheses, structural determination, and binding studies of nine-coordinate mononuclear $(mnH)_2[Dy^{III}(Httha)]\cdot 3H_2O$ and $(enH_2)_3[Dy^{III}(ttha)]_2\cdot 9H_2O$

YUAN BAI [a], JINGQUN GAO [a], JUN WANG [a], XUDONG JIN [a], TONG WU [a] & YUMEI KONG [a]

[a] Institute of Inorganic Chemistry, College of Chemistry, Liaoning University, Shenyang, P.R. China

Accepted author version posted online: 12 Dec 2012.Published online: 29 Jan 2013.

To cite this article: YUAN BAI, JINGQUN GAO, JUN WANG, XUDONG JIN, TONG WU & YUMEI KONG (2013) Syntheses, structural determination, and binding studies of nine-coordinate mononuclear $(mnH)_2[Dy^{III}(Httha)]\cdot 3H_2O$ and $(enH_2)_3[Dy^{III}(ttha)]_2\cdot 9H_2O$, Journal of Coordination Chemistry, 66:3, 367-378, DOI: 10.1080/00958972.2012.757600

To link to this article: http://dx.doi.org/10.1080/00958972.2012.757600

Journal of Coordination Chemistry
Vol. 66, No. 3, 10 February 2013, 367–378

Syntheses, structural determination, and binding studies of nine-coordinate mononuclear $(mnH)_2[Dy^{III}(Httha)]\cdot 3H_2O$ and $(enH_2)_3[Dy^{III}(ttha)]_2\cdot 9H_2O$

YUAN BAI, JINGQUN GAO, JUN WANG*, XUDONG JIN, TONG WU and YUMEI KONG

Institute of Inorganic Chemistry, College of Chemistry, Liaoning University, Shenyang, P.R. China

(*Received 14 January 2012; in final form 11 October 2012*)

Two dysprosium coordination compounds, $(mnH)_2[Dy^{III}(Httha)]\cdot 3H_2O$ (**1**) (H_6ttha = triethylenetetramine-N,N,N′,N″,N‴,N⁗-hexaacetic acid and mn = methylamine) and $(enH_2)_3[Dy^{III}(ttha)]_2\cdot 9H_2O$ (**2**) (en = ethylenediamine), were synthesized through direct heating and characterized by elemental analysis, FT-IR, thermal analysis, and single-crystal X-ray diffraction. X-ray diffraction analysis displays that **1** is a mononuclear nine-coordinate complex with a pseudo-monocapped square antiprismatic conformation (MCSAP) crystallizing in the monoclinic crystal system with *P*2(1)/c space group. The crystal data are as follows: $a = 16.1363(19)$ Å, $b = 13.9336(11)$ Å, $c = 13.6619(14)$ Å, $\beta = 102.2490(10)°$, and $V = 3001.8(5)$ Å^3. There are two kinds of methylamine cation in **1**. They connect $[Dy^{III}(Httha)]^{2-}$and crystal waters through hydrogen bonds, leading to formation of a 2-D ladder-like layer structure. The polymeric **2** also is a nine-coordinate structure with a pseudo-MCSAP crystallizing in the monoclinic crystal system with *P*2/c space group. The cell dimensions are: $a = 17.7801(16)$ Å, $b = 9.7035(10)$ Å, $c = 22.096(2)$ Å, $\beta = 118.874(2)°$, and $V = 3338.3(6)$ Å^3. In **2** there are also two types of ethylenediamine cations. One connects three adjacent $[Dy^{III}(ttha)]^{3-}$ complex anions through hydrogen bonds and the other is symmetrical forming hydrogen bonds with two neighboring $[Dy^{III}(ttha)]^{3-}$ complex anions. These hydrogen bonds result in formation of a 2-D ladder-like layer structure as well.

Keywords: Dysprosium ion (Dy^{III}); Triethylenetetramine-N,N,N′,N″,N‴,N⁗-hexaacetic acid (H_6ttha); Methylamine (mn); Ethylenediamine (en); Hydrogen bond

1. Introduction

Design and synthesis of rare-earth metal complexes have attracted a great deal of attention for flexible coordination geometry and potential applications in catalysis, gas storage, magnetism, optics, etc. [1–5]. The Tb^{III} complexes are generally used as fluorescence probes in diagnosing certain diseases [6]. The Er^{III} complexes have been taken as functional materials for optical telecommunication networks [7–9]. The element $^{153}Sm^{III}$ with favorable chemistry and physical characteristics, such as half-life of 46.27 h and β- and γ-emissions with moderate energy, has attracted much attention, widely used for tumor therapy of brain, liver, lung, heart, and bone tissues [10–12]. The Pr^{III} complexes in

*Corresponding author. Email: wangjuncomplex890@126.com

ISSN 0095-8972 print/ISSN 1029-0389 online
http://dx.doi.org/10.1080/00958972.2012.757600

solids show outstanding optical features [13,14]. The Dy^{III} complexes have antibacterial activities and reduce blood sugar levels [15]. With desirable physical characteristics and availability, Dy^{III} complexes have been used for palliative treatment of pain from metastatic bone cancer, radiation synovectomy, and radioimmunotherapy [16–18]. The importance of Dy^{III} complexes in biology activities encourages us to study the molecular structure of Dy^{III} complexes.

A series of Dy^{III} complexes have been reported by our laboratory, $K_3[Dy^{III}(ttha)]\cdot 5H_2O$ (H_6ttha = triethylenetetramine-N,N,N′,N″,N‴,N‴-hexaacetic acid) [19–21], $(NH_4)_3[Dy^{III}(ttha)]\cdot 5H_2O$ [22], $K_3[Dy^{III}(nta)_2(H_2O)]\cdot 5H_2O$ (H_3nta = nitrilotriacetic acid) [23], $Na_3[Dy^{III}(nta)_2(H_2O)]\cdot 5.5H_2O$ [24], and $(NH_4)_3[Dy^{III}(nta)_2]$ [23]. By comparative analysis, we found that Dy^{III} complexes are of eight or nine coordinates in pseudo-monocapped square antiprismatic, dicapped trigonal antiprismatic, or tricapped trigonal prismatic geometries. Our studies show that their coordination numbers and structures sometimes relate to counter ion species. Ammonium ion has a certain impact on structures of rare-earth complexes with aminocarboxylate ligands. We want to know how the organic amine affects coordination number, coordinate structure, space group, molecular structure, and crystal atructure. In addition, because the organic amine can be regarded as the part of amino acids, interactions between organic amines with rare-earth complex anions is significant for the exploration of their bioactivities.

We decided to prepare new rare-earth complexes using organic amines as counter ions. In this work, we chose methylamine and ethylenediamine as counter ions and synthesized $(mnH)_2[Dy^{III}(Httha)]\cdot 3H_2O$ (**1**) (mn = methylamine) and $(enH_2)_3[Dy^{III}(ttha)]_2\cdot 9H_2O$ (**2**) (en = ethylenediamine). Single-crystal X-ray diffraction reveals that both are nine-coordinate structures. However, due to different counter ions, **1** and **2** have some differences in crystal structure, space group, etc. Therefore, organic amines affect not only molecular structure, but also space group and crystal structure.

2. Experimental

2.1. *Syntheses*

2.1.1. $(mnH)_2[Dy^{III}(Httha)]\cdot 3H_2O$ (1). H_6ttha (= triethylenetetramine-N,N,N′,N″,N‴, N‴-hexaacetic acid) (A.R., Beijing SHLHT Science & Trade Co., Ltd., China) (2.4723 g, 5.0 mmol) was added to 100 ml warm water and Dy_2O_3 powder (99.999%, Yuelong Rare Earth Co., Ltd., China) (0.9325 g, 2.5 mmol) was added slowly to the above solution. After the mixture had been stirred and refluxed for 15.0 h, the solution became transparent, and then the pH was adjusted to 6.0 by dilute methylamine (mn) aqueous solution. Finally, the solution was concentrated to 25 ml. White crystals appeared after three weeks at room temperature. Yield is 3.08 g. In the elemental analyzes, C, H, and N were determined by a THERMO flash EA 1112 type analyzer instrument and the Dy^{III} was analyzed by oxalate titration and thermal analysis. Anal. Found (%): Dy – 21.20, C – 31.14, H – 5.59, and N – 10.89; Calcd (%): Dy – 21.10, C – 31.16, H – 5.58, and N – 10.91.

2.1.2. $(enH_2)_3[Dy^{III}(ttha)]_2\cdot 9H_2O$ (2). H_6ttha (A.R., Beijing SHLHT Science & Trade Co., Ltd., China) (2.4723 g, 5.0 mmol) was added to 100 ml warm water and Dy_2O_3 powder (99.999%, Yuelong Rare Earth Co., Ltd., China) (0.9325 g, 2.5 mmol) was added

to the above solution slowly. The solution became transparent after the mixture had been stirred and refluxed for 15.0 h. Then the pH was also adjusted to 6.0 by dilute ethylenediamine (en) aqueous solution and concentrated to 25 ml. Yellow crystals appeared after three weeks at room temperature. Yield is 3.30 g. Elemental analyzes of complex were carried out by adopting the same methods as mentioned above. Anal. Found (%): Dy – 19.61, C – 30.56, H – 5.85, and N – 11.84; Calcd (%): Dy – 19.69, C – 30.54, H – 5.82, and N – 11.88.

2.2. *FT-IR spectra determination*

The H_6ttta, $(mnH)_2[Dy^{III}$ (Httha)]·$3H_2O$ and $(enH_2)_3[Dy^{III}$ (ttha)]$_2$·$9H_2O$ samples were skived and pressed to slices with KBr and their infrared spectra (IR) were recorded by a Shimadzu-IR 408 spectrograph. The results are shown in figure S1.

2.3. *Determination of TG-DTA*

Thermal analysis of **1** and **2** were conducted using a Mettler-Toledo 851° thermogravimetric analyzer in a flow of Ar (20 mL min^{-1}) from room temperature to 800 °C at a heating rate of 10 °C min^{-1}; thermograms are shown in figure S2.

2.4. *X-ray structure determination*

X-ray intensity data were collected on a Bruker SMART CCD type X-ray diffractometer system with graphite-monochromated Mo Kα radiation ($\lambda = 0.71073$ Å) at 298 K using φ–ω scan technique from $1.72° \leqslant \theta \leqslant 26.00°$. The structure was solved by direct methods. All nonhydrogen atoms were refined anisotropically by full-matrix least-squares on F^2. All calculations were performed by the SHELXTL-97 program on PDP11/44 and Pentium MMX/166 computers. Figures 1 and S3 illustrate the perspective views of **1** and **2**, respectively. Figures 2 and S4 show their coordination polyhedra. Figures 3 and 6 display their molecular packing in a unit cell and figures 4 and 7 present the inner hydrogen bonds. Figure 5 and figure 8 give the extended 2-D ladder-like structures of **1** and **2**. Crystal data and structure refinements for **1** and **2** are listed in table 1 and selected bond distances and angles in table 2. Final atomic coordinates and equivalent isotropic displacement parameters for all the nonhydrogen fractions are presented in table S1. Hydrogen bond distances and angles of **1** and **2** are listed in table S2.

3. Results and discussion

3.1. *FT-IR Spectra*

3.1.1. $(mnH)_2[Dy^{III}$(Httha)]·$3H_2O$ (1). Comparison of FT-IR spectra between H_6ttha and **1**, shown in figure S1(a and b), reveals that $\nu_{(C–N)}$ of **1** is at 930 cm^{-1}. Compared with $\nu_{(C–N)}$ of H_6ttha at 899 cm^{-1}, $\nu_{(C–N)}$ of **1** displays a blue shift (31 cm^{-1}), which demonstrates that the amine nitrogen of H_6ttha coordinates to Dy^{III}. In addition, **1** gives characteristic absorptions of carboxyl groups at 1601 cm^{-1} for the asymmetric stretch and at 1406 cm^{-1} for the symmetric stretch, indicating that oxygens of carboxyl groups are also coordinated to Dy^{III}. The presence of an absorption at 1736 cm^{-1} reveals that there is

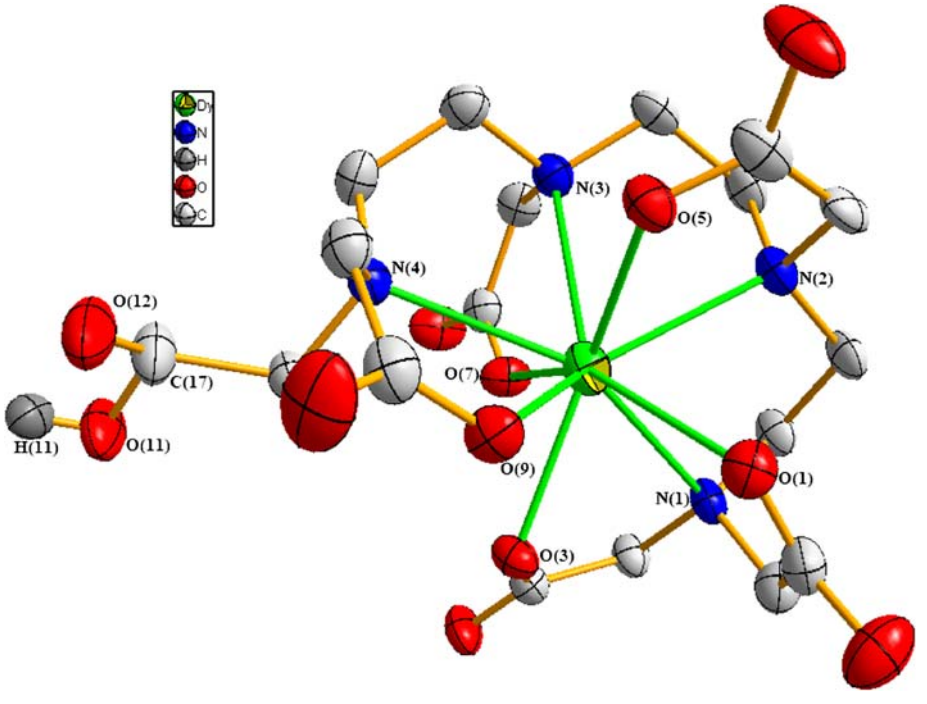

Figure 1. Molecular structure of **1**.

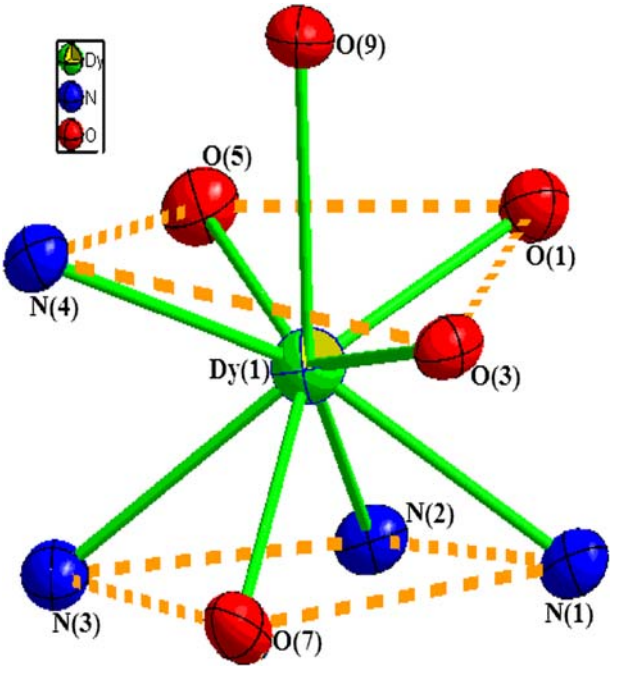

Figure 2. Coordination polyhedron around Dy(1) in compound **1**.

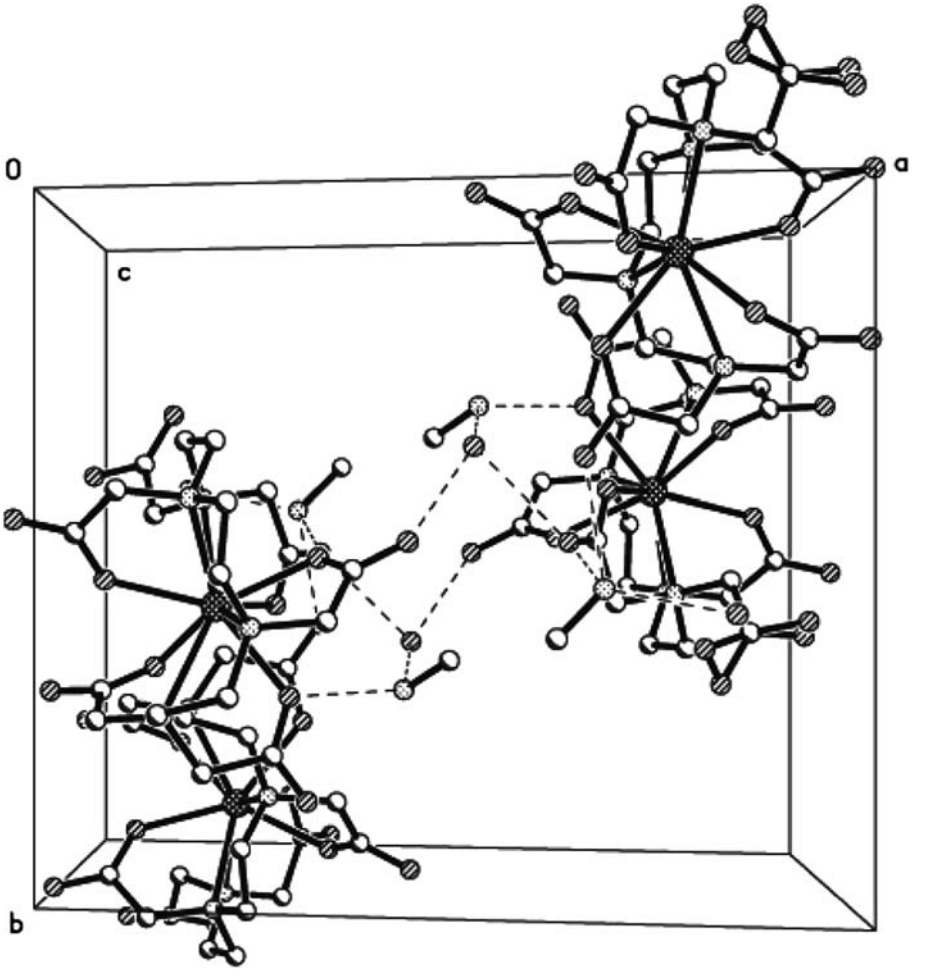

Figure 3. Arrangement of **1** in the unit cell (dashed lines represent intermolecular hydrogen bonds).

a noncoordinate carboxylic group in **1**. There is a broad absorption band around 3421 cm^{-1} for **1**, attributed to stretch of O–H bond.

3.1.2. $(enH_2)_3[Dy^{III}(ttha)]_2 \cdot 9H_2O$ (2). As shown in figure S1(c), the $\nu_{(C-N)}$ of **2** at 935 cm^{-1} also displays a blue shift (36 cm^{-1}) indicating that amine nitrogens of H_6ttha are coordinated to Dy^{III}. The characteristic absorptions of carboxyls at 1590 cm^{-1} for asymmetric stretch and at 1412 cm^{-1} for symmetric stretch indicate oxygens of carboxyl are coordinated to Dy^{III}. The absence of strong absorption at 1736 cm^{-1} reveals that all carboxylic groups are completely deprotonated, consistent with the results of X-ray diffraction analyzes. A strong and broad absorption at 3421 cm^{-1} shows existence of O–H bond in **2**.

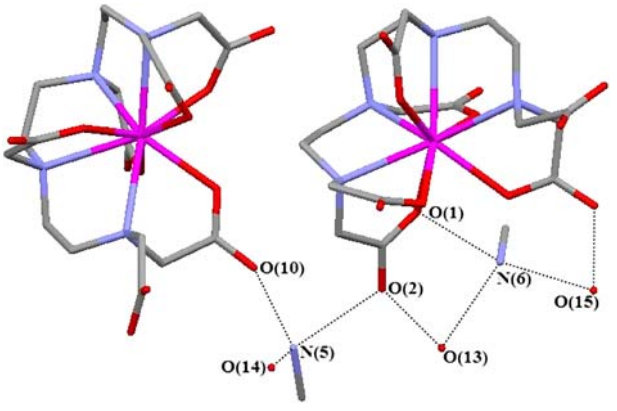

Figure 4. Bindings between mnH^+ and $[Dy^{III}(Httha)]^{2-}$ in **1** (dashed lines represent intermolecular hydrogen bonds).

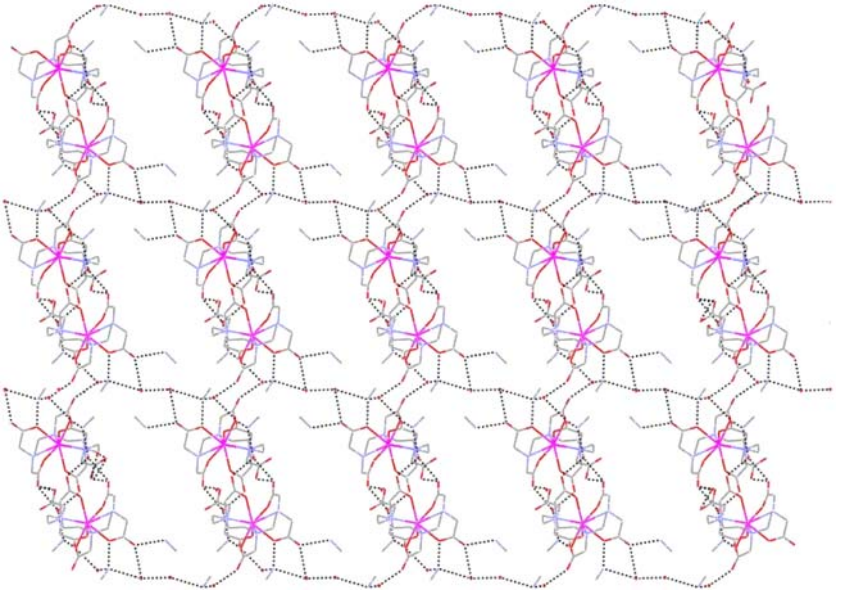

Figure 5. Polyhedral view of the 2-D ladder-like layered network of **1**.

3.2. *Thermal analysis*

3.2.1. $(mnH)_2[Dy^{III}(Httha)]\cdot 3H_2O$ (1). As shown in figure S2, the TG curve of **1** shows a five-stage decomposition. The first stage of 3.9% from room temperature to 98 °C with an endothermic peak at 90 °C in the differential thermal analysis (DTA) curve corresponds to expulsion of one methylamine. The second weight loss of 5.5% from 98 to 210 °C with an obvious endothermic peak at 151 °C corresponds to the expulsion of one methylamine and one crystal water. The third stage weight loss attributed to the expulsion of remaining crystal water is from 210 to 260 °C. The weight loss ratio is 4.6%. In the

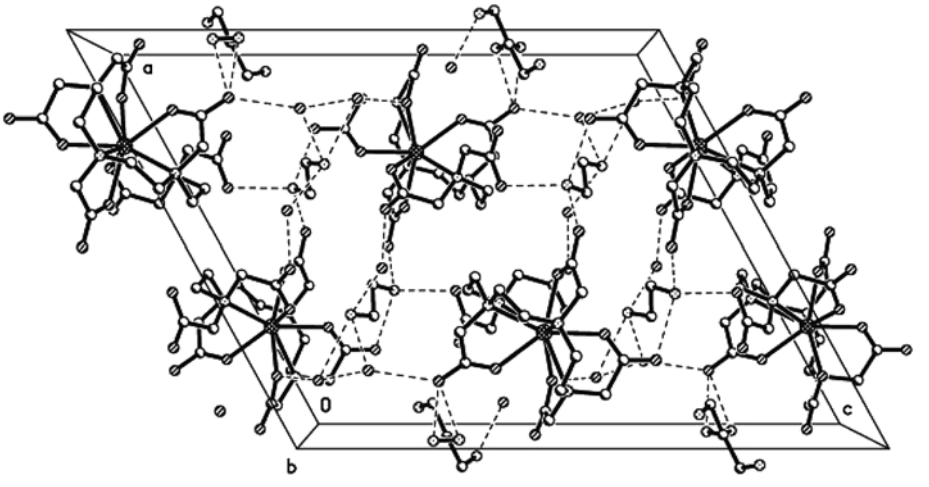

Figure 6. Arrangement of compound $(enH_2)_3[Dy^{III}(ttha)]2{\cdot}9H_2O$ (**2**) in the unit cell (dashed lines represent intermolecular hydrogen bonds).

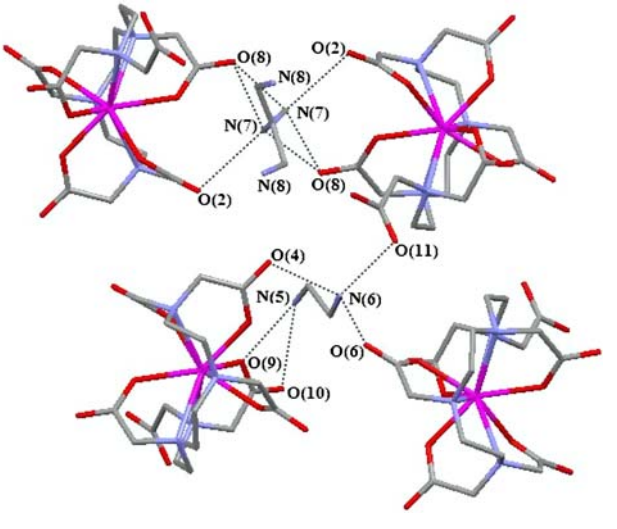

Figure 7. Bindings between enH_2^{2+} and $[Dy^{III}(ttha)]^{3-}$ in **2** (dashed lines represent intermolecular hydrogen bonds).

DTA curve, there is an endothermic peak at 217 °C. The fourth stage weight loss of 20.4% from 260 to 370 °C is attributed to decomposition of carboxylates, with an endothermic peak at 269 °C. The last stage from 370 to 800 °C (weight loss of 23.3%) corresponds to combustion of the sample; the remainder is Dy_2O_3. The total weight loss ratio is about 57.7% according to the mass calculation.

3.2.2. $(enH_2)_3[Dy^{III}(ttha)]_2{\cdot}9H_2O$ (2). The thermal decomposition of **2** is similar to that of **1**, but with only four stages. The first thermal decomposition happens from 25 to

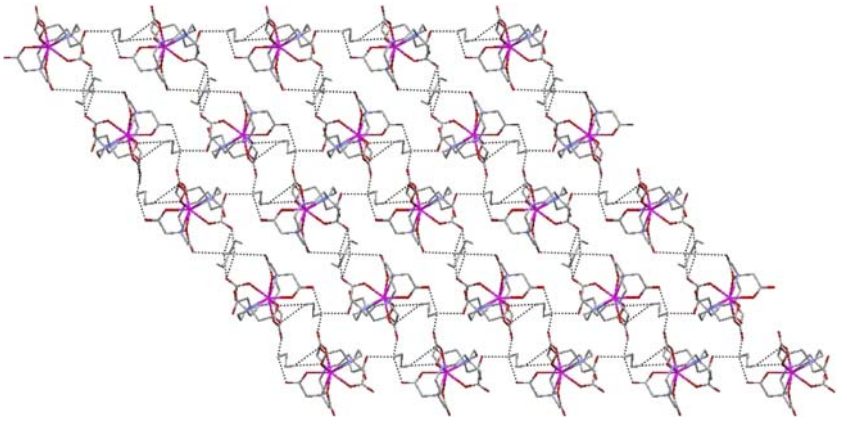

Figure 8. Polyhedral view of the 2-D ladder-like layered network of **2**.

Table 1. Crystal data and structure refinement for **1** and **2**.

Complex	**1**	**2**
Empirical formula	$C_{20}H_{43}DyN_6O_{15}$	$C_{42}H_{96}Dy_2N_{14}O_{33}$
Formula weight	770.10	1650.33
Temperature, K	298(2)	298(2)
Wavelength, Å	0.71073	0.71073
Crystal system	Monoclinic	Monoclinic
Space group	$P2_1/c$	$P2/c$
Unit cell dimensions		
a, Å	16.1363(19)	17.7801(16)
b, Å	13.9336(11)	9.7035(10)
c, Å	13.6619(14)	22.096(2)
β, deg	102.2490(10)	118.874(2)
Volume, Å^3	3001.8(5)	3338.3(6)
Z	4	2
ρ_{calcd}, Mg m^{-3}	1.704	1.642
Absorption coefficient, mm^{-1}	2.567	2.318
$F(0\,0\,0)$	1564	1684
Crystal size, mm	$0.45 \times 0.41 \times 0.30$	$0.40 \times 0.32 \times 0.21$
θ_{range} for data collection, °	2.30 to 25.02	2.43 to 25.02
Limiting indices	$-19 \leqslant h \leqslant 17$ $-13 \leqslant k \leqslant 16$ $-13 \leqslant l \leqslant 16$	$-20 \leqslant h \leqslant 21$ $-11 \leqslant k \leqslant 11$ $-26 \leqslant l \leqslant 26$
Reflections collected	15,013	16,252
Independent reflections	5300 [R(int) = 0.0386]	5890 [R(int) = 0.0386]
Completeness to θ_{max}, %	99.9	99.8
Max. and min. transmission	0.5131 and 0.3913	0.6417 and 0.4574
Goodness-of-fit on F^2	1.054	1.071
Final R indices [$I > 2\sigma(I)$]	$R_1 = 0.0311$, $wR_2 = 0.0742$	$R_1 = 0.0514$, $wR_2 = 0.1415$
R indices (all data)	$R_1 = 0.0421$, $wR_2 = 0.0788$	$R_1 = 0.0789$, $wR_2 = 0.1697$
Largest diff. peak and hole, e Å^{-3}	1.355 and −1.006	1.847 and −1.268
Absorption correction	Empirical	
Refinement method	Full-matrix least-squares on F^2	

220 °C, producing a DTA peak at 136 °C with weight loss of 7.8%, corresponding to two ethylenediamines. The second weight loss (13.6%) from 220 to 320 °C with an endothermic peak at 268 °C corresponds to expulsion of nine crystal waters. The third stage weight

Table 2. Selected bond distances (Å) and angles (°) of **1** and **2**.

Bond	*d* (Å)	Bond	*d* (Å)	Bond	*d* (Å)
1					
Dy(1)–O(1)	2.364(3)	Dy(1)–O(7)	2.320(3)	Dy(1)–N(2)	2.621(3)
Dy(1)–O(3)	2.359(3)	Dy(1)–O(9)	2.387(3)	Dy(1)–N(3)	2.714(4)
Dy(1)–O(5)	2.336(3)	Dy(1)–N(1)	2.612(3)	Dy(1)–N(4)	2.635(3)
2					
Dy(1)–O(1)	2.389(7)	Dy(1)–O(7)	2.322(6)	Dy(1)–N(2)	2.634(8)
Dy (1)–O(3)	2.330(6)	Dy(1)–O(9)	2.351(6)	Dy(1)–N(3)	2.715(8)
Dy(1)–O(5)	2.352(6)	Dy(1)–N(1)	2.625(8)	Dy(1)–N(4)	2.652(6)
Angle	ω, deg	Angle	ω, deg	Angle	ω, deg
1					
O(1)–Dy(1)–O(3)	84.99(10)	O(3)–Dy(1)–N(2)	132.61(10)	O(7)–Dy(1)–N(3)	64.05(10)
O(1)–Dy(1)–O(5)	77.24(10)	O(3)–Dy(1)–N(3)	134.23(10)	O(7)–Dy(1)–N(4)	76.68(11)
O(1)–Dy(1)–O(7)	141.93(11)	O(3)–Dy(1)–N(4)	92.24(10)	O(9)–Dy(1)–N(1)	121.05(10)
O(1)–Dy(1)–O(9)	70.77(10)	O(5)–Dy(1)–O(7)	136.16(11)	O(9)–Dy(1)–N(2)	133.17(10)
O(1)–Dy(1)–N(1)	66.59(10)	O(5)–Dy(1)–O(9)	75.12(10)	O(9)–Dy(1)–N(3)	125.72(10)
O(1)–Dy(1)–N(2)	74.39(11)	O(5)–Dy(1)–N(1)	129.00(10)	O(9)–Dy(1)–N(4)	65.58(10)
O(1)–Dy(1)–N(3)	138.29(10)	O(5)–Dy(1)–N(2)	67.35(10)	N(1)–Dy(1)–N(2)	69.06(10)
O(1)–Dy(1)–N(4)	135.24(10)	O(5)–Dy(1)–N(3)	72.46(11)	N(1)–Dy(1)–N(3)	113.21(11)
O(3)–Dy(1)–O(5)	148.14(10)	O(5)–Dy(1)–N(4)	82.51(10)	N(1)–Dy(1)–N(4)	148.20(10)
O(3)–Dy(1)–O(7)	71.52(10)	O(7)–Dy(1)–O(9)	126.98(10)	N(2)–Dy(1)–N(3)	67.87(11)
O(3)–Dy(1)–O(9)	74.12(10)	O(7)–Dy(1)–N(1)	76.11(10)	N(2)–Dy(1)–N(4)	132.10(11)
O(3)–Dy(1)–N(1)	63.61(10)	O(7)–Dy(1)–N(2)	99.70(10)	N(3)–Dy(1)–N(4)	67.97(11)
2					
O(1)–Dy(1)–O(3)	84.8(2)	O(3)–Dy(1)–N(2)	73.5(3)	O(7)–Dy(1)–N(3)	64.4(2)
O(1)–Dy(1)–O(5)	149.2(2)	O(3)–Dy(1)–N(3)	137.4(2)	O(7)–Dy(1)–N(4)	76.3(2)
O(1)–Dy(1)–O(7)	70.9(2)	O(3)–Dy(1)–N(4)	137.0(2)	O(9)–Dy(1)–N(1)	122.9(3)
O(1)–Dy(1)–O(9)	74.2(2)	O(5)–Dy(1)–O(7)	136.5(2)	O(9)–Dy(1)–N(2)	135.4(2)
O(1)–Dy(1)–N(1)	63.2(3)	O(5)–Dy(1)–O(9)	76.9(2)	O(9)–Dy(1)–N(3)	125.2(2)
O(1)–Dy(1)–N(2)	131.5(2)	O(5)–Dy(1)–N(1)	128.2(3)	O(9)–Dy(1)–N(4)	64.3(2)
O(1)–Dy(1)–N(3)	134.4(2)	O(5)–Dy(1)–N(2)	66.7(2)	N(1)–Dy(1)–N(2)	68.3(3)
O(1)–Dy(1)–N(4)	93.6(2)	O(5)–Dy(1)–N(3)	72.4(2)	N(1)–Dy(1)–N(3)	111.8(3)
O(3)–Dy(1)–O(5)	77.3(2)	O(5)–Dy(1)–N(4)	83.1(2)	N(1)–Dy(1)–N(4)	148.0(2)
O(3)–Dy(1)–O(7)	140.9(2)	O(7)–Dy(1)–O(9)	124.6(2)	N(2)–Dy(1)–N(3)	67.4(2)
O(3)–Dy(1)–O(9)	74.0(2)	O(7)–Dy(1)–N(1)	75.4(2)	N(2)–Dy(1)–N(4)	131.6(2)
O(3)–Dy(1)–N(1)	66.3(2)	O(7)–Dy(1)–N(2)	99.8(2)	N(3)–Dy(1)–N(4)	67.8(2)

loss (28.1%) from 320 to 408 °C is attributed to decomposition of carboxylate accompanied with an endothermic peak at 392 °C. The last stage from 408 to 800 °C (weight loss of 14.1%) corresponds to combustion of the sample with the final product of Dy_2O_3. The total weight loss ratio is about 63.6% according to the mass calculation.

3.3. *Molecular and crystal structures*

3.3.1. $(mnH)_2[Dy^{III}(Httha)]\cdot 3H_2O$ (1). Figure 1 shows the nine-coordinate structure of **1** with 1 : 1 Dy^{III} to H_6ttha. It is similar to $K_4[Eu_2^{III}(Httha)_2]\cdot 13.5H_2O$ [25] and $Na_2[Tb^{III}(Httha)]\cdot 6H_2O$ [26]. The central Dy^{III} is coordinated with four amine nitrogens and five oxygens, all coming form one H_6ttha ligand. This nine-coordinate complex contains a noncoordinated carboxyl group (–CH_2COOH), very important because it may be modified by functional groups or biological molecules to become a specific target drug with great diagnostic and therapeutic effect.

The coordinate geometry around Dy^{III} ion can be considered as nine-coordinate distorted monocapped square antiprismatic conformation (MCSAP). In the atoms coordinated to Dy^{III}, the set of O(1), O(3), O(5), and N(4) and the set of O(7), N(1), N(2), and N(3) form two approximate square planes, which form a square antiprism. The capping donor is O(9). The torsion angle between the two quadrilateral planes is about 41.86°.

Based on figure 2, it can also be calculated that, for the top plane, the value of trigonal dihedral angle is 14.80° between Δ(O(5)O(3)O(1)) and Δ(O(5)O(3)N(4)) and 15.08° between Δ(O(1)N(4)O(3)) and Δ(O(1)N(4)O(5)). For the bottom plane, the trigonal dihedral angle between Δ(N(2)O(7)N(1)) and Δ(N(2)O(7)N(3)) is about 5.91° and between Δ(N(1)N(3)N(2)) and Δ(N(1)N(3)O(7)) is about 6.94°. According to Guggenberger and Muetterties [27], the structures can be regarded as a pseudo-monocapped square antiprism if the dihedral angle for nine-coordinate lanthanide complexes is between 0°–26.4°. So, we confirm that $\{DyN_4O_5\}$ in $[Dy^{III}(Httha)]^{2-}$ is a pseudo-MCSAP.

As shown in table 2, the Dy(1)–O bond distances vary from 2.320(3) Å (Dy(1)–O(7)) to 2.387(3) Å (Dy(1)–O(9)) and the average value is 2.353(5) Å; the Dy(1)–N bond lengths range between 2.612(3) Å (Dy(1)–N(1)) and 2.714(4) Å (Dy(1)–N(3)) with an average value of 2.645(8) Å. The Dy(1)–O bond distances are significantly shorter than the Dy(1)–N bond distances suggesting that Dy(1)–O bonds are more stable than Dy(1)–N bonds.

The O–Dy–O bond angles range from 70.77(10)° (O(1)–Dy(1)–O(9)) to 148.14(10)° (O(3)–Dy(1)–O(5)), while the O–Dy–N bond angles vary from 63.61(10)° (O(3)–Dy(1)–N(1)) to 138.29(10)° (O(1)–Dy(1)–N(3)). The largest and smallest bond angles are 148.14(10)° (O(3)–Dy(1)–O(5)) and 63.61(10)° (O(3)–Dy(1)–N(1)), respectively. The reason might be that the O(3) forms hydrogen bond with the adjacent crystal water.

As shown in figure 3, there are four $(mnH)_2[Dy^{III}(Httha)]\cdot 3H_2O$ molecules in a unit cell. The complex molecules connect with crystal water and protonated methylamine cations (mnH^+) through hydrogen bonds and crystallize in a monoclinic system with $P2_1/c$ space group. There are two kinds of mnH^+, one mnH^+ is N(5)–C(19) (figure 4). Each N(5) connects with three oxygens, in which O(2) and O(10) are uncoordinated carboxyl from two $[Dy^{III}(Httha)]^{2-}$ complex anions and O(14) from one crystal water. Hydrogen bond distances of N(5)···O(2), N(5)···O(10) and N(5)···O(14) are 2.745, 2.753, and 2.741 Å, respectively. The second mnH^+ is N(6) which links one carboxyl O (O(1)) from $[Dy^{III}(Httha)]^{2-}$ and O(13) and O(15) from two crystal waters. The N(6)···O(1), N(6)···O(13) and N(6)···O(15) hydrogen bond distances are 2.841, 2.909, and 2.729 Å, respectively.

Shown in figure 5, every two $[Dy^{III}(Httha)]^{2-}$ are interconnected by methylamine (N(5)–C(19)) and water (O(14)), forming a basic secondary building unit (SBU). Hydrogen bond distances of N(5)···O(10), N(5)···O(14), and O(14)···O(8) are 2.753, 2.741, and 2.742 Å, respectively. Two neighboring SBUs are further connected by sharing methylamine (N(6)–C(20)) and water O(13) along the *a*-axis, with O(1)···N(6), O(13)···N(6), and O(13)···O(2) hydrogen bond distances of 2.841, 2.909, and 13.734 Å, respectively, resulting in an infinite 1-D chain. 1-D chains connect to another chain by waters and methylamines along the *b*-axis leading to a loose 2-D ladder-like network structure.

3.3.2. $(enH_2)_3[Dy^{III}(ttha)]_2\cdot 9H_2O$ (2). As seen from figure S3, **2** has similar building units with **1** although en is counter ion. It also is similar to $(enH_2)_3[Eu^{III}(ttha)]_2\cdot 11H_2O$ [28] and $(enH_2)_{1.5}[Sm^{III}(ttha)]\cdot 4.5H_2O$ [29]. The central Dy^{III} is of nine coordinates in a distorted pseudo-monocapped square antiprism (shown in figure S4) with eight-coordinate atoms forming two approximate parallel planes. The average torsion angle of two square

planes is 41.66°. The capping donor is occupied by O(9) under the upper plane formed by O(1), O(3), O(5), and N(4). The lengths of Dy(1)–O bonds (seen from table 2) are slightly different, with average value of 2.349(4) Å. Dy(1)–N bond lengths have a mean value of 2.657(3) Å. The O–Dy–O bond angles are 70.9(2)° (O(1)–Dy(1)–O(7)) to 149.2(2)° (O(1)–Dy(1)–O(5)). The O–Dy–N bond angles vary from 63.2(3)° (O(1)–Dy(1)–N(1)) to 137.4(2)° (O(3)–Dy(1)–N(3)) and the N–Dy–N bond angles change from 67.4(2)° (N(2)–Dy(1)–N(3)) to 148.0(2)° (N(1)–Dy(1)–N(4)). The upper quadrilateral plane has a dihedral angle between Δ(O(1)O(3)O(5)) and Δ(O(1)O(5)N(4)) of 13.78°, and between Δ(O(1)O(3)N(4)) and Δ(O(3)O(5)N(4)) of 13.85°. To the bottom plane, the corresponding value is 5.32° between triangle Δ(N(1)N(2)N(3)) and Δ(O(7)N(1)N(3)), and 4.58° between Δ(O(7)N(1)N(2)) and Δ(O(7)N(2)N(3)). The coordination structure of $\{DyN_2O_7\}$ in $[Dy^{III}(ttha)]^{3-}$ keeps a pseudo-monocapped square antiprismatic polyhedron.

There are two $(enH_2)_3[Dy^{III}(ttha)]_2\cdot 9H_2O$ molecules in a unit cell (figure 6) crystallizing in a monoclinic system with *P*2/c space group, not exactly the same as $(mnH)_2[Dy^{III}(ttha)]\cdot 3H_2O$. There are two types of enH_2^{2+} (figure 7), one enH_2^{2+} forms hydrogen bonds with three adjacent $[Dy^{III}(ttha)]^{3-}$ complex anions and the second enH_2^{2+}, which is highly symmetric, forms hydrogen bonds with two adjacent $[Dy^{III}(ttha)]^{3-}$. As shown in figure 8, every two $[Dy^{III}(ttha)]^{3-}$ are interconnected by sharing the highly symmetric ethylenediamine (N(7)–C(21)–C(22)–N(8)) along the *c*-axis with hydrogen bond distances for N(7)···O(8), N(7)···O(2) and N(7)···O(8) of 2.774, 3.049, and 2.715 Å, respectively. The dihedral angle of ethylenediamine is 172.99°. Two neighboring $[Dy^{III}(ttha)]^{3-}$ are further connected by sharing two ethylenediamines (N(5)–C(19)–C(20)–N(6)) along the *a*-axis, with N(5)···O(9), N(5)···O(10), N(6)···O(4), N(6)···O(6) and N(6)···O(11) hydrogen bond distances of 3.017, 2.980, 2.803, 2.756 and 2.745 Å, respectively, resulting in formation of infinite 1-D chains. Two 1-D chains are linked by sharing ethylenediamine (N(5)–C(19)–C(20)–N(6)) in the *ac* plane leading to formation of a close-knit 2-D ladder-like network.

4. Conclusions

Two Dy^{III} complexes with H_6ttha (= triethylenetetramine-N,N,N′,N″,N‴,N‴-hexaacetic acid), $(mnH)_2[Dy^{III}(Httha)]\cdot 3H_2O$ (**1**) (mn = methylamine), and $(enH_2)_3[Dy^{III}(ttha)]_2\cdot 9H_2O$ (**2**) (en = ethylenediamine) were synthesized by direct heating and characterized by elemental analysis, FT-IR spectrum, thermal analysis, and single-crystal X-ray diffraction. The compound **1** is a mononuclear nine-coordinate complex with monocapped square antiprismatic polyhedron crystallizing in the monoclinic crystal system with $P2_1/c$ space group. Besides being different from previously reported $K_3[Dy^{III}(ttha)]\cdot 5H_2O$ and $(NH_4)_3[Dy^{III}(ttha)]\cdot 5H_2O$, the use of methylamine as the counter ion results in formation of a noncoordinate carboxyl group (–CH_2COOH) in **1**; **2** also has a nine-coordinate pseudo-MCSAP crystallizing in the monoclinic crystal system with *P*2/c space group, but $[Dy^{III}(ttha)]^{3-}$ anions make up a 2-D ladder-like network structure through connection of enH_2^{2+}, different from $K_3[Dy^{III}(ttha)]\cdot 5H_2O$ and $(NH_4)_3[Dy^{III}(ttha)]\cdot 5H_2O$. The FT-IR spectra and thermal analyses support the results of single-crystal X-ray diffraction. Changes of FT-IR absorptions of carboxyl and amine prove that some oxygens and nitrogens coordinate to Dy^{III}. In thermal analyses, because of enH_2^{2+}, **2** displays slightly higher thermal stability than the **1**. Particularly, by referring to the research results in recent years, it once again shows that the molecular structure, coordinate conformation as well as crystal structure of

rare-earth metal complexes with aminopolycarboxylic acid ligands are related to the counter ions.

Supplementary material

CCDC 859472 for $(mnH)_2[Dy^{III}(Httha)]\cdot H_2O$ and CCDC 859471 for $(enH_2)_3[Dy^{III}(ttha)]_2\cdot 9H_2O$ contain the supplementary crystallographic data for this article. These data can be obtained free of charge via http://www.ccdc.cam.ac.uk/data_request/cif, by emailing data_request@ccdc.cam.ac.uk, or by contacting The Cambridge Crystallographic Data Center, 12 Union Road, Cambridge CB2 1EZ, UK; Fax:+44(0)1223-336033.

Acknowledgments

The authors greatly acknowledge the National Natural Science Foundation of China, Liaoning Province, Natural Science Foundation of Education Department, Liaoning Province, Natural Science Foundation of Science and Technology Department and Liaoning University "211" project for financial support. The authors also thank our colleagues and other students for their participation in this work. Especially, we thank Professor K. Miyoshi and T. Mizuta (Faculty of Science, Hiroshima University, Japan) for instruction.

References

[1] C. Janiak. *Dalton Trans.*, 2781 (2003).
[2] A.J. Chmura, M.G. Davidson, M.D. Jones, M.D. Lunn, M.F. Mahon. *Dalton Trans.*, 887 (2006).
[3] C.J. Kepert. *Chem. Commun.*, **7**, 695 (2006).
[4] D. Maspoch, D.R. Molina, J. Veciana. *Chem. Soc. Rev.*, **36**, 770 (2007).
[5] K. Kuriki, Y. Koike, Y. Okamoto. *Chem. Rev.*, **102**, 2347 (2002).
[6] D. Parker. *Coord. Chem. Rev.*, **205**, 109 (2000).
[7] Q. Wang, N.K. Dutta, R. Ahrens. *J. Appl. Phys.*, **95**, 4025 (2004).
[8] R.G. Sun, Y.Z. Wang, Q.B. Zheng. *J. Appl. Phys.*, **87**, 7589 (2000).
[9] P.G. Kik, M.L. Brongersma, A. Polman. *Appl. Phys. Lett.*, **76**, 2325 (2000).
[10] W.A. Volkert, T.J. Hoffman. *Chem. Rev.*, **99**, 2269 (1999).
[11] G.J. Beyer, R. Offord, G. Künzi, Y. Aleksandrova, U. Ravn, J. Barker, O. Tengblad, M. Lindroos. *Nucl. Med. Biol.*, **24**, 367 (1997).
[12] M. Neves, L. Gano, N. Pereira, M.R. Costa, M. Chabdia, M. Rosado, R. Fausto. *Nucl. Med. Biol.*, **29**, 329 (2002).
[13] J.Y. Niu, J.W. Zhao, J.P. Wang. *Inorg. Chem. Commun.*, **7**, 876 (2004).
[14] J.B. Yu, H.J. Zhang, L.S. Fu, R.P. Deng, L. Zhou, H.R. Li, F.Y. Liu, H.L. Fu. *Inorg. Chem. Commun.*, **6**, 852 (2003).
[15] Z.J. Chen, X.L. Liu. *Rare Earths*, **22**, 68 (2001).
[16] C. Kremer, J. Torres, S. Dominguez, A. Mederos. *Coord. Chem. Rev.*, **249**, 567 (2005).
[17] W.A. Volkert, W.F. Goeckeler, G.J. Ehrhardt, A.R. Ketring. *J. Nucl. Med.*, **32**, 174 (1991).
[18] W.P. Li, D.S. Ma, C. Higginbotham, T. Hoffman, A.R. Ketring, S.S. Jurisson. *Nucl. Med. Biol.*, **28**, 145 (2001).
[19] J. Wang, Y. Wang, Z.H. Zhang, X.D. Zhang, X.Y. Liu, Z.R. Liu, Y. Zhang, J. Tong, P. Zhang. *J. Coord. Chem.*, **59**, 295 (2006).
[20] D.F. Chen, W.C. Yang, R.Y. Wang, T.Z. Jin. *Acta Chim. Sinica*, **55**, 672 (1997).
[21] J. Wang, X.D. Zhang, R. Ma. *Chem. Res. Chin. Univ.*, **18**, 237 (2002).
[22] J. Wang, X.D. Zhang, W.G. Jia, H.F. Li, B.X. Ren. *J. Chin. Rare Earth Soc.*, **20**, 7 (2002).
[23] J. Wang, X.Z. Liu, H. Zhang, X.D. Zhang, G.R. Gao, Y.M. Kong, Y. Li. *J. Coord. Chem.*, **47**, 906 (2006).
[24] J. Wang, G.R. Gao, Z.H. Zhang, X.D. Zhang, Y.J. Wang. *J. Coord. Chem.*, **60**, 2221 (2007).
[25] J. Wang, X.D. Zhang, Y. Zhang, Y. Wang, X.Y. Liu, Z.R. Liu. *Russ. J. Coord. Chem.*, **30**, 850 (2004).
[26] B. Liu, Y.F. Wang, J. Wang, J. Gao, R. Xu, Y.M. Kong, L.Q. Zhang, X.D. Zhang. *Russ. J. Coord. Chem.*, **50**, 917 (2009).
[27] L.J. Guggenberger, E.L. Muetterties. *J. Am. Chem. Soc.*, **98**, 7221 (1976).
[28] R. Xu, D. Li, J. Wang, Y.X. Kong, B.X. Wang, Y.M. Kong, T.T. Fan, B. Liu. *Russ. J. Coord. Chem.*, **36**, 810 (2010).
[29] J.Q. Gao, D. Li, J. Wang, X.D. Jin, T. Wu, K. Li, P.L. Kang, X.D. Zhang. *J. Coord. Chem.*, **64**, 2234 (2011).